

## Crystal Structure of $Zn_xCd_{1-x}S$ Nanocrystals Obtained by Self-Propagating High-Temperature Synthesis

A.V. Kovalenko, Ye.G. Plakhtii, O.V. Khmelenko

Oles Honchar Dnipro National University, 72, Gagarin Ave., 49010 Dnipro, Ukraine

(Received 12 April 2021; revised manuscript received 23 February 2022; published online 28 February 2022)

$Zn_xCd_{1-x}S$  nanocrystals were obtained by self-propagating high-temperature synthesis. The synthesis was carried out in an air environment at atmospheric pressure. We managed to synthesize nanocrystals close to CdS ( $0 \leq x < 0.2$ ), as well as close to ZnS ( $0.8 \leq x \leq 1$ ) by changing the ratio between Zn and Cd from 0 to 1 with a step of 0.1 in a real product. Their sizes were determined by the Scherrer method and were in the range of  $40\text{--}60 \pm 5$  nm.  $Zn_xCd_{1-x}S$  nanocrystals of all compositions were characterized by a mixed crystal structure; the maximum proportion of the cubic phase was typical of compositions close to ZnS, and the minimum one – of compositions close to CdS. The degrees of microdeformations of the crystal lattice of  $Zn_xCd_{1-x}S$  nanocrystals were within  $1.05 \cdot 10^{-4}\text{--}3.97 \cdot 10^{-3}$ ; dislocation densities were determined within  $7.91 \cdot 10^{10}\text{--}3.1 \cdot 10^{11}$ . Based on the analysis of the EPR spectra, it was shown that when the local environment of  $Mn^{2+}$  ions changed with increasing parameter  $x$ , the constant of the EPR hyperfine structure of  $Mn^{2+}$  ions explosively decreased from the value  $A = 7.00\text{--}7.06$  mT to the value  $A = 6.84$  mT. The presence of the EPR line of  $Cr^{3+}$  ions in unlit ZnS and  $Zn_{0.8}Cd_{0.2}S$  nanocrystals may indirectly indicate  $n$ -type conductivity of the samples obtained.

**Keywords:**  $Zn_xCd_{1-x}S$  nanocrystals, Zinc sulfide, Cadmium sulfide, Self-propagating high-temperature synthesis, X-ray diffraction analysis, EPR spectra, Crystal structure.

DOI: [10.21272/jnep.14\(1\).01017](https://doi.org/10.21272/jnep.14(1).01017)

PACS numbers: 81.20.Ka, 76.30. – v, 61.05.cp

### 1. INTRODUCTION

Wide-band gap  $A_2B_6$  compounds hold a special place among the semiconductor materials. They are characterized by high radiation, temperature and mechanical resistance. LEDs, lasers, sensors of the gas content of the medium have been created on the basis of these materials [1-3]. Some of the most popular representatives of  $A_2B_6$  compounds are zinc and cadmium sulfide with various activators, as well as compounds of  $Zn_xCd_{1-x}S$  solid solution, where the electrical and optical properties can be changed over a wide range by changing width of the band gap. Therefore, these compounds are one of the most important materials for the creation of solar cells, photodetectors, nonlinear optical devices, etc. [4-6]. Additional interest in these compounds arises in connection with the widespread use of nanocrystals (NCs) in various optoelectronic emitting structures [7, 8] as well as nanosensors [9, 10]. Therefore, the development of effective technologies for obtaining  $Zn_xCd_{1-x}S$  NCs with reproducible and controllable properties is an urgent technological problem.

Self-propagating high-temperature synthesis (SHS), also known as the combustion method, has a number of advantages in the list of various methods for producing  $A_2B_6$  type NCs. The advantages of this method are the high speed of production of the final product ( $\sim 3\text{--}5$  s), the possibility of obtaining NCs in large volumes, low cost and energy consumption per unit of production, the simplicity of the equipment used and its environmental safety [11]. Due to SHS method, powdery  $Zn_xCd_{1-x}S$  NCs can be obtained from a mixture of fine-dispersed Zn, Cd and S powders, and they can be doped directly in the synthesis process by adding appropriate impurities to the charge. It should be noted that ZnS [12], ZnS:Mn [13, 14], CdS [15],  $Zn_xSe_{1-x}$  [16, 17] NCs were previously obtained by SHS method. However, accord-

ing to our data,  $Zn_xCd_{1-x}S$  and  $Zn_xCd_{1-x}S:Mn$  NCs have not been synthesized by this method yet. This work is devoted to the analysis of the peculiarities of obtaining  $Zn_xCd_{1-x}S$  and  $Zn_xCd_{1-x}S:Mn$  NCs by SHS method, as well as the results of studies of their physical properties by X-ray diffraction analysis (XRD) and EPR.

### 2. METHODOLOGY OF EXPERIMENT

Synthesis of NCs of  $Zn_xCd_{1-x}S$  and  $Zn_xCd_{1-x}S:Mn$  solid solutions was carried out in a quartz ampoule placed in a sealed steel reactor. The ampoule was loaded with mechanically mixed powders of Zn, Cd, and S taken in appropriate proportions. Preliminary mixing of the charge was carried out with the addition of ethyl alcohol to improve the mixing process. The ratio of Zn and Cd in the charge was characterized by the parameter  $x_p$ . The synthesis reaction was initiated by a heat pulse after drying the mixture. It was provided by a nichrome spiral located in the upper part of the reactor, when a current pulse with an amplitude of  $\sim 35$  A and a duration of  $\sim 1$  s passed through it. The synthesis was carried out at atmospheric pressure in air. The ratio between Zn and Cd was determined by the parameter  $x$ , which differed from the parameter  $x_p$  in the obtained  $Zn_xCd_{1-x}S$  NCs. In order to determine the parameter  $x$  in  $Zn_xCd_{1-x}S$  NCs according to XRD data, we used Vegard's law, which establishes a linear change in the crystal lattice parameters with a change in the ratio between Zn and Cd cations in  $Zn_xCd_{1-x}S$  solid solutions [18]. Consequently, it was shown that the parameter  $x$  in the synthesized  $Zn_xCd_{1-x}S$  NCs differs significantly from the parameter  $x_p$ . The relationship between these parameters is shown in Fig. 1a. It should be emphasized that by changing the parameter  $x_p$  from 0 to 1 with a step of 0.1 in a real product, we were able to synthesize  $Zn_xCd_{1-x}S$  NCs close to CdS ( $0 \leq x < 0.2$ ), as

well as close to ZnS ( $0.8 \leq x \leq 1$ ). Thus, when using SHS method,  $Zn_xCd_{1-x}S$  NCs are efficiently synthesized in such compositions when the number of cations of one type significantly exceeds the concentration of cations of another type. Doping of  $Zn_xCd_{1-x}S$  NCs with  $Mn^{2+}$  ions was carried out by adding  $10^{-2}$  wt. % of  $MnCl_2$  salt

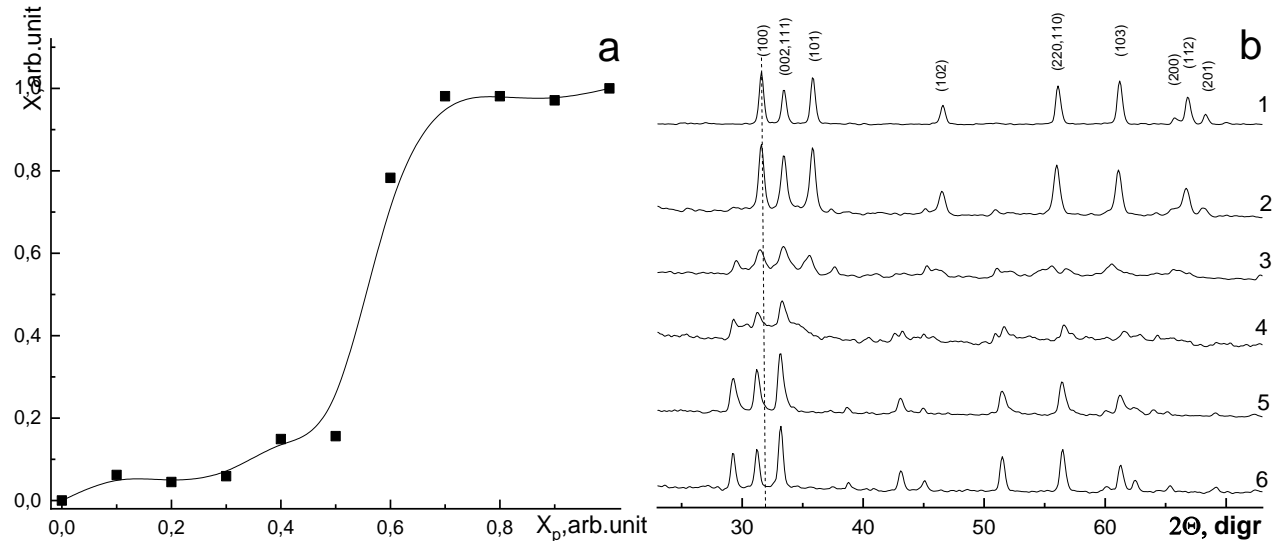
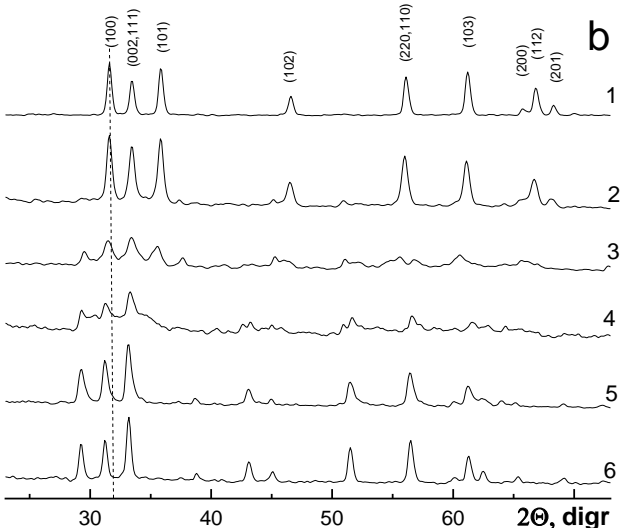


**Fig. 1 – Dependence of the parameter  $x$  in  $Zn_xCd_{1-x}S$  NCs on the parameter  $x_p$  (a); XRD data (b) of NCs at  $x_p = 1$  (1), 0.8 (2), 0.6 (3), 0.4 (4), 0.2 (5), 0 (6)**

### 3. EXPERIMENTAL RESULTS AND DISCUSSION

$Zn_xCd_{1-x}S$  NCs obtained by SHS method were powders, whose form is shown in Fig. 2. The XRD data and analysis of the EPR spectra in  $Zn_xCd_{1-x}S$  NCs show that NCs with the same parameter  $x$  differ from each other depending on which parameter  $x_p$  was inserted into the initial charge for synthesis. So, for example,  $Zn_xCd_{1-x}S$  NCs with  $x \sim 1$ , synthesized from a charge with  $x_p = 0.7 \pm 1$  (Fig. 1a), were characterized by significant differences in the EPR spectra data, sizes of NCs, the

to the initial charge. XRD of the obtained NCs was performed with a DRON-2 diffractometer using Co-K $\alpha$  radiation. EPR spectra were investigated with a Radio-pen SE/X-2543 radio spectrometer. Images of NC particles were obtained using a scanning electron microscope REMMA-102-02.



ratio of cubic and hexagonal phases, and the degree of microdeformation. In this regard, when analyzing the obtained results, we will operate with the parameter  $x_p$ , despite the fact that the parameter  $x$  may be the same for NCs in the final product. The synthesized powders of  $Zn_xCd_{1-x}S$  compounds consisted of polycrystals with a mixed crystal structure and an average size of 1-5 μm, which, in turn, consisted of NCs. Their sizes were determined by the Scherrer method and found for  $x_p = 0 \pm 0.3$  and  $0.7 \pm 1$  in the range of  $60 \pm 5$  nm, and for the parameter  $x_p = 0.4 \pm 0.6$  in the range of  $40 \pm 5$  nm (Fig. 3a).

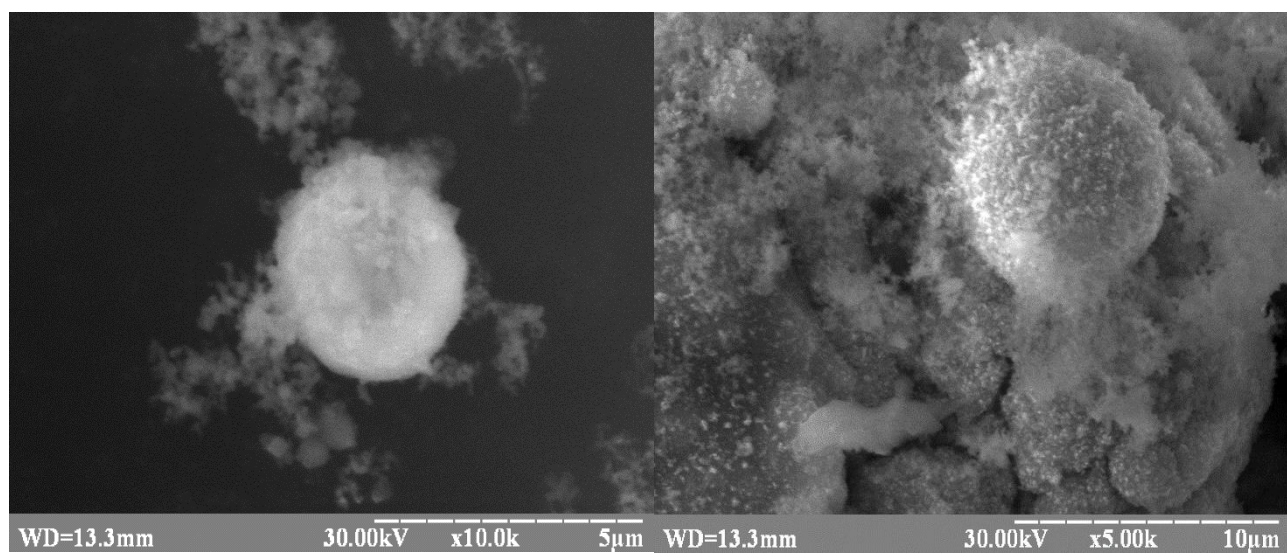


**Fig. 2 – Surface morphology of  $Zn_xCd_{1-x}S$  NCs with parameter  $x_p = 1$  (a) and  $x_p = 0.2$  (b)**

The minimum sizes of  $Zn_xCd_{1-x}S$  NCs are typical for the parameter  $x_p = 0.4$ , and the maximum sizes – for compositions with the parameters  $x_p = 0$  and  $x_p = 1$ .

In NC with the parameter  $x_p = 1$ , the part of the hexagonal phase was  $\sim (65 \pm 5)\%$ , the cubic phase was  $\sim (35 \pm 5)\%$ ; in NC with the parameter  $x_p = 0.6$ , these parts were  $(75 \pm 5)\%$  and  $(25 \pm 5)\%$ ; in NC with the parameter  $x_p = 0.4$ , they were  $(80 \pm 5)\%$  and  $(20 \pm 5)\%$ ; in NC with the parameter  $x_p = 0$ , the part of the hexagonal phase was  $\sim (85 \pm 5)\%$  and the part of the cubic one was

$\sim (15 \pm 5)\%$ . Thus, with a decrease in the parameter  $x_p$ , the proportion of the hexagonal phase in  $Zn_xCd_{1-x}S$  NCs increased, and the proportion of the cubic phase correspondingly decreased. It should be noted that the hexagonal phase prevails in CdS NCs, which is not typical for bulk CdS crystals. An abrupt change in the ratio of hexagonal and cubic phases in  $Zn_xCd_{1-x}S$  NCs is characteristic of the compositions with  $x_p = 0.4 \div 0.6$  in this case (Fig. 3b).

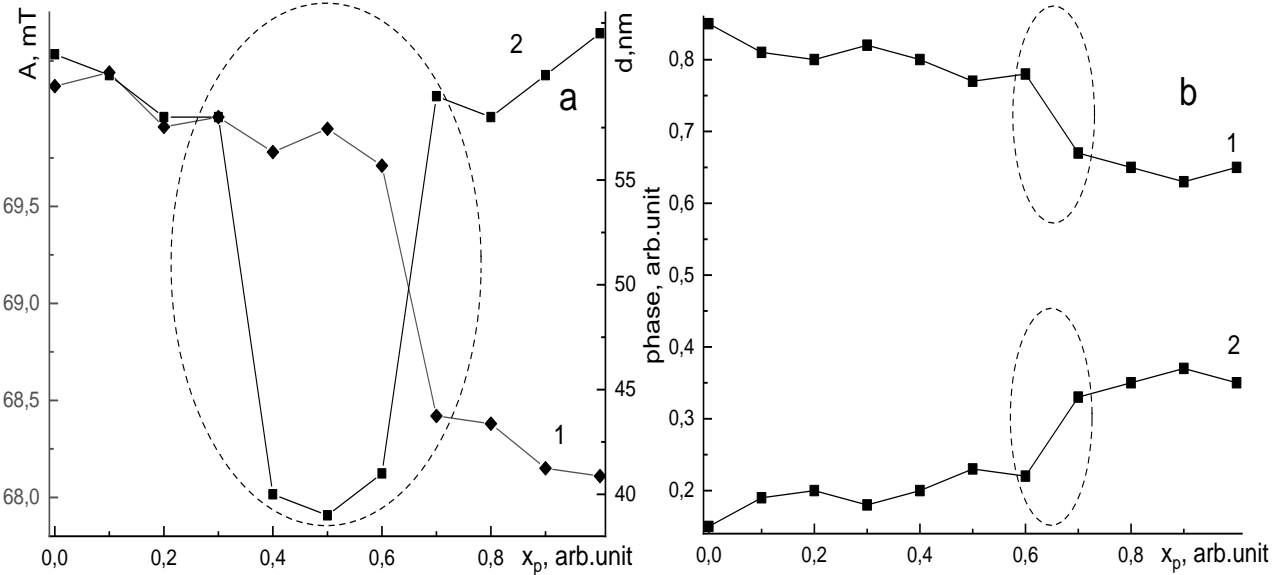


**Fig. 3** – Dependence of the hyperfine structure constant  $A$  (a) of the EPR spectra of  $Mn^{2+}$  ions (1) and the sizes of NCs (2); dependences (b) of the parts of hexagonal (1) and cubic (2) phases in  $Zn_xCd_{1-x}S$  NCs on the parameter  $x_p$ . The dotted lines mark the areas of abrupt changes in these dependences

The crystal lattice parameters of NCs of  $Zn_xCd_{1-x}S$  solid solutions in the hexagonal phase vary from  $a = 3.805 \text{ \AA}$  and  $c = 6.238 \text{ \AA}$  (for  $x = 1$ ) to  $a = 4.127 \text{ \AA}$  and  $c = 6.693 \text{ \AA}$  (for  $x = 0$ ). These values differ from the crystal lattice parameters of single crystals of  $Zn_xCd_{1-x}S$  solid solutions [19], which are in the range from  $a = 3.794 \text{ \AA}$  and  $c = 6.268$  (for  $x = 1$ ) to  $a = 4.121 \text{ \AA}$  and  $c = 6.682 \text{ \AA}$  (for  $x = 0$ ), which may be associated with the deformation stresses characteristic of NCs. The degree of microdeformation of the crystal lattice of  $Zn_xCd_{1-x}S$  NC ( $\Delta a/a$ ) is determined in the range from  $1.05 \cdot 10^{-4}$  (for  $x_p = 0$ ) to  $3.97 \cdot 10^{-3}$  (for  $x_p = 0.4$ ), and the dislocation density ranges from  $7.91 \cdot 10^{10}$  (for  $x_p = 0$ ) to  $3.1 \cdot 10^{11}$  (for  $x_p = 0.4$ ), respectively.

A hyperfine structure, consisted of six equidistant lines characteristic of paramagnetic  $Mn^{2+}$  ions, is observed in the EPR spectra of self-activated  $Zn_xCd_{1-x}S$  NCs of all compositions (Fig. 4a). These lines turned out to be doubled in compositions with  $x_p = 1$ , which indicates the superposition of two EPR spectra. One of them with a hyperfine structure constant  $A = 7.15 \text{ mT}$  belongs to  $Mn^{2+}$  ions located in a hexagonal local environment. Another spectrum with a hyperfine structure constant  $A = 6.88 \text{ mT}$  is conditional on  $Mn^{2+}$  ions in a cubic environment. This result correlates with the RDA data, which established the presence of a mixed crystal structure in ZnS NC. The EPR lines of  $Mn^{2+}$  ions are low-intensity in compositions with  $0.4 \leq x_p \leq 0.6$ , which

indicates that  $Mn^{2+}$  ions are poorly incorporated into the crystal lattice of NCs in such compositions. As mentioned earlier, this range of values of the parameter  $x_p$  is characterized by a large-scale rearrangement of the crystal structure. The ratios between hexagonal and cubic phases, the NC size and the value of the hyperfine structure constant  $A$  for  $Mn^{2+}$  ions change abruptly in this range (Fig. 3). The intensity of the EPR spectra of  $Mn^{2+}$  ions increases significantly in compositions close to CdS ( $x_p \leq 0.2$ ). The value of the constant for these spectra was  $A \sim 6.82 \div 6.84 \text{ mT}$ , which is typical for  $Mn^{2+}$  ions located in the hexagonal structure of CdS [20].

Weak lines were also observed in the EPR spectra of ZnS NCs, which are marked by a dotted line in Fig. 4a. These lines can be associated with forbidden transitions, which were previously observed in other works [14]. Probably their appearance is due to a strong deformation of the crystal lattice, as well as numerous dangling chemical bonds on the surface, which are characteristic of NC. In addition, a single EPR line with  $g = 1.9998$  conditional on  $Cr^{2+}$  ions was recorded in ZnS NC. These centers are formed as a result of electron capture by  $Cr^{2+}$  ions, which isovalently substitute for  $Zn^{2+}$  ions in the ZnS crystal lattice. Typically, such a line is recorded in zinc sulfide under UV excitation. The appearance of such a signal in unlit NCs may indirectly indicate that ZnS NCs have  $n$ -type conductivity.

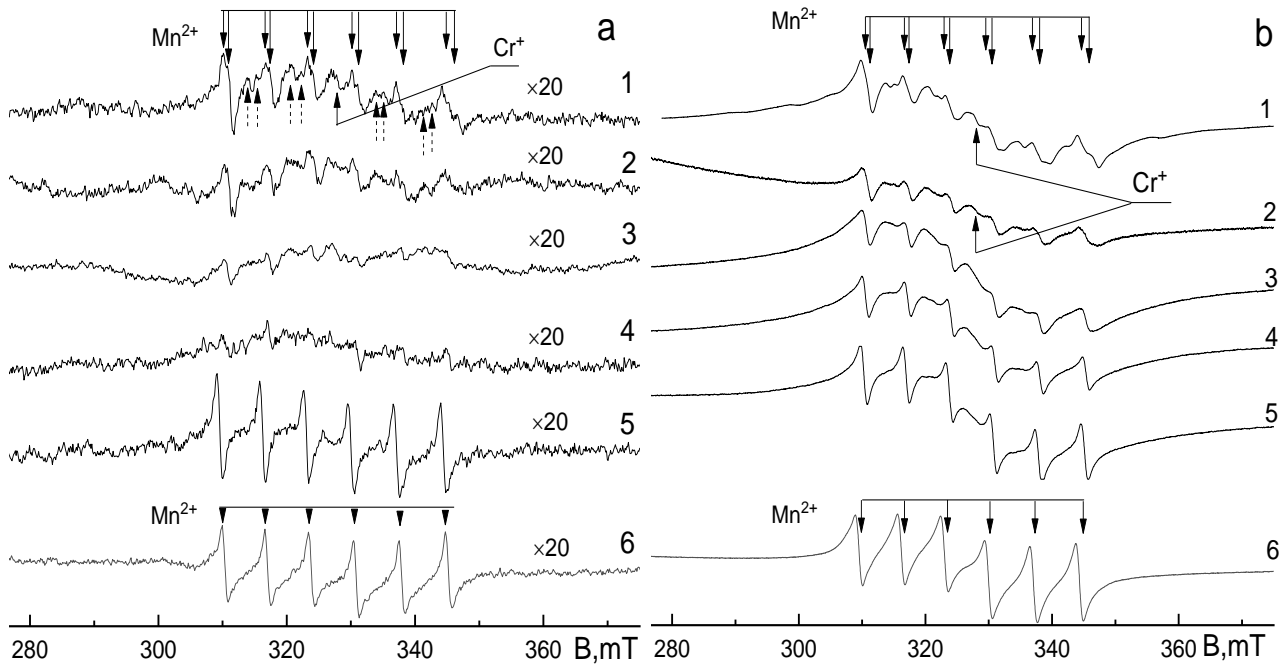


**Fig. 3 – EPR spectrum of  $Zn_xCd_{1-x}S$  (a) and  $Zn_xCd_{1-x}S:Mn$  (b) NCs at  $x_p = 1$  (1), 0.8 (2), 0.6 (3), 0.4 (4), 0.2 (5), 0 (6)**

The intensity and width of the EPR lines of  $Mn^{2+}$  ions increase significantly in doped  $Zn_xCd_{1-x}S:Mn$  NCs (Fig. 4b). Compositions  $0.8 \leq x_p \leq 1$  also contain a single EPR line caused by  $Cr^{3+}$  ions. We could not reliably detect this signal for other values of the parameter  $x_p$ . This fact may indicate that, as the parameter  $x_p$  decreases, the strongly pronounced *n*-type conductivity characteristic of ZnS NCs gradually shifts to *p*-type conductivity, which, in turn, makes it difficult to form EPR centers associated with  $Cr^{3+}$  ions.

#### 4. CONCLUSIONS

NCs of  $Zn_xCd_{1-x}S$  and  $Zn_xCd_{1-x}S:Mn$  solid solutions were obtained by SHS method. The ratio between Zn and Cd (parameter  $x_p$ ) varied from 0 to 1 with a step of 0.1 in the initial charge. The ratio between Zn and Cd (parameter  $x$ ) was determined based on Vegard's law in the final product, which allowed establishing of the dependence of the parameter  $x$  on the parameter  $x_p$ . The sizes of NCs were within  $60 \pm 5$  nm for compositions

with  $x_p = 0 \div 0.3$  and  $0.7 \div 1$  and within  $40 \pm 5$  nm for the parameter  $x_p = 0.4 \div 0.6$ . It was shown that this method can be used to obtain ternary compounds close to ZnS and CdS with parameters  $x = 0.8 \div 1$  and  $x = 0 \div 0.2$ . NCs of all compositions are characterized by a mixed crystal structure; the maximum fraction of the cubic phase is characteristic of compositions close to ZnS, and the minimum one is characteristic of compositions close to CdS. According to the EPR data, in compositions with a parameter value of  $0.7 < x_p \leq 1$   $Mn^{2+}$  ions are locally surrounded by sulfur ions, which are most likely in the cubic phase. In compositions with  $x_p \leq 0.7$ ,  $Mn^{2+}$  ions are locally surrounded by sulfur ions in the hexagonal phase. Simultaneously with a change in the local environment of  $Mn^{2+}$  ions, the EPR hyperfine structure constant of  $Mn^{2+}$  ions changes abruptly from  $A = 7.00 \div 7.06$  mT to  $A = 6.84$  mT. The presence of a single EPR line of  $Cr^{3+}$  ions in unlit  $Zn_xCd_{1-x}S$  NCs with  $0.9 \leq x_p \leq 1$  may indirectly indicate *n*-type conductivity of the obtained samples.

#### REFERENCES

- C.J. Panchal, A.S. Opanasyuk, V.V. Kosyak, M.S. Desai, I.Yu. Protsenko, *J. Nano-Electron. Phys.* **3**, 274 (2011).
- H.E. Ruda, *Widegap II-VI compounds for opto-electronic applications* (Springer Science & Business Media: 2013).
- S.V. Ivanov, S.V. Sorokin, I.V. Sedova, *Mater. Sci. Forum*, **571** (2018).
- X. Xu, R. Lu, X. Zhao, S. Xu, X. Lei, F. Zhang, D.G. Evans, *Appl Catal B-Environ* **102**, 147 (2011).
- G.V. Colibaba, E.V. Monaco, E.P. Gonçalves, D.D. Nedeoglo, I.M. Tiginyanu, K. Nielsch, *Semicond. Sci. Tech.* **29** No 12, 125003 (2014).
- R. Zia, F. Saleemi, S. Naseem, Z. Kayani, *Ener. Rep.* **1**, 58 (2015).
- O. Wang, L. Wang, Z. Li, Q. Xu, Q. Lin, H. Wang, L.S. Li, *Nanoscale* **10**, 5650 (2018).
- M. Yang, Y. Wang, Y. Ren, E. Liu, J. Fan, X. Hu, *J. Alloy Compd.* **752**, 260 (2018).
- J. Konyukhova, A. Skaptsov, E. Volkova, V. Galushka, V. Kochubey, *Saratov Fall Meeting 2013* **9031**, 90310L (2014).
- E. Volkova, A. Skaptsov, J. Konyukhova, V. Kochubey, M. Kozintseva, *Saratov Fall Meeting 2014* **9448**, 94480V (2015).
- E.A. Levashov, A.S. Mukasyan, A.S. Rogachev, D.V. Shtansky, *Int. Mater. Rev.* **62**, 203 (2016).
- S.V. Kozitskii, V.P. Pisarskii, O.O. Ulanova, *Combust. Explos. Shock*, **34**, 34 (1998).
- Y.Y. Bacherikov, N.P. Baran, I.P. Vorona, A.V. Gilchuk, A.G. Zhuk, Y.O. Polishchuk, N.E. Korsunska, *J. Mater. Sci.: Mater. Electron.* **28**, 8569 (2017).
- M.F. Bulaniy, A.V. Kovalenko, A.S. Morozov, O.V. Khmelenko,

- J. Nano-Electron. Phys.*, **9**, 2007-1 (2017).
15. A.D. Mani, N. Xanthopoulos, D. Laub, C.H. Subrahmanyam, *J. Chem. Sci.* **126**, 967 (2014).
16. A.V. Kovalenko, Y.G. Plakhtii, O.V. Khmelenko, *Funct. Mater.* **25**, 665 (2018).
17. A.V. Kovalenko, Y.G. Plakhtii, O.V. Khmelenko, *J. Nano-Electron. Phys.* **11**, 04031 (2019).
18. Y. Zhang, J. Cai, T. Ji, Q. Wu, Y. Xu, X. Wang, Z. Hu, *Nano Res.* **8**, 584 (2015).
19. Z. Wang, L.L. Daemen, Y. Zhao, C.S. Zha, R.T. Downs, X. Wang, R. J. Hemley, *Nat. Mater.* **4**, 922 (2005).
20. B. Sambandam, T. Muthukumar, S. Arumugam, P.L. Paulose, P.T. Manoharan, *RSC Adv.* **4**, 22141 (2014).

## Кристалічна структура нанокристалів Zn<sub>x</sub>Cd<sub>1-x</sub>S, отриманих шляхом саморозповсюдженого високотемпературного синтезу

А.В. Коваленко, Є.Г. Плахтій, О.В. Хмеленко

*Дніпровський національний університет імені Олеся Гончара, пр. Гагаріна, 72, 49010 Дніпро, Україна*

Нанокристали Zn<sub>x</sub>Cd<sub>1-x</sub>S були отримані методом саморозповсюдженого високотемпературного синтезу. Синтез проводили в повітряному середовищі за атмосферного тиску. Нам вдалося синтезувати нанокристали, близькі до CdS ( $0 \leq x < 0,2$ ), а також близькі до ZnS ( $0,8 \leq x \leq 1$ ), змінюючи співвідношення Zn і Cd з 0 до 1 з кроком 0,1 у реальному продукті. Їх розміри визначали за методом Шеррера і знаходилися в межах  $40 \pm 60 \pm 5$  нм. Нанокристали Zn<sub>x</sub>Cd<sub>1-x</sub>S усіх складів характеризувались змішаною кристалічною структурою; максимальна частка кубічної фази характерна для складів, близьких до ZnS, а мінімальна – для складів, близьких до CdS. Ступені мікродеформації кристалічної решітки нанокристалів Zn<sub>x</sub>Cd<sub>1-x</sub>S були в межах  $1,05 \cdot 10^4 \div 3,97 \cdot 10^3$ ; густину дислокаций визначали в межах  $7,91 \cdot 10^{10} \div 3,1 \cdot 10^{11}$ . На основі аналізу спектрів ЕПР було показано, що при зміні локального оточення іонів Mn<sup>2+</sup> із збільшенням параметра  $x$  константа надтонкої структури ЕПР іонів Mn<sup>2+</sup> стрибкоподібно змінювалася від значення  $A = 7,00 \pm 7,06$  мТ до значення  $A = 6,84$  мТ. Наявність лінії ЕПР іонів Cr<sup>+</sup> у неосвітлених нанокристалах ZnS та Zn<sub>0,8</sub>Cd<sub>0,2</sub>S може побічно вказувати на провідність *n*-типу отриманих зразків.

**Ключові слова:** Нанокристали Zn<sub>x</sub>Cd<sub>1-x</sub>S, Сульфід цинку, Сульфід кадмію, Саморозповсюджуваний високотемпературний синтез, Рентгеноструктурний аналіз, Спектри ЕПР, Кристалічна структура.